

## Mesoscale Eddies Influence Coral Reef Environments in the Northwest Gulf of Mexico

**Key Points:**

- Argo floats can be used to study open ocean eddies that translate physical and biogeochemical conditions over the continental shelf-edge
- Eddies increase the range of thermal variability within Flower Garden Banks National Marine Sanctuary half of the days in each month
- Mixed layer depth changes seasonally and within eddies, influencing temperature and salinity ranges over the reef

**Supporting Information:**

Supporting Information may be found in the online version of this article.

**Correspondence to:**

J. K. McWhorter,  
Jennifer.mcwhorter@noaa.gov

**Citation:**

McWhorter, J. K., Roman-Stork, H. L., Le Hénaff, M., Frenzel, H., Johnston, M. A., Cornec, M., & Osborne, E. (2024). Mesoscale eddies influence coral reef environments in the northwest Gulf of Mexico. *Journal of Geophysical Research: Oceans*, 129, e2023JC020821. <https://doi.org/10.1029/2023JC020821>

Received 13 DEC 2023








Accepted 16 MAY 2024

**Author Contributions:**

**Conceptualization:** J. K. McWhorter, M. Le Hénaff, E. Osborne  
**Data curation:** J. K. McWhorter, H. L. Roman-Stork, H. Frenzel, M. Cornec  
**Formal analysis:** J. K. McWhorter, H. L. Roman-Stork, M. Le Hénaff, E. Osborne  
**Funding acquisition:** E. Osborne  
**Investigation:** J. K. McWhorter, H. L. Roman-Stork, M. Le Hénaff, E. Osborne  
**Methodology:** J. K. McWhorter, M. Le Hénaff, H. Frenzel, E. Osborne  
**Project administration:** J. K. McWhorter, E. Osborne

© 2024. The Author(s).

This is an open access article under the terms of the [Creative Commons Attribution License](#), which permits use, distribution and reproduction in any medium, provided the original work is properly cited.

J. K. McWhorter<sup>1</sup> , H. L. Roman-Stork<sup>2,3</sup> , M. Le Hénaff<sup>1,4</sup> , H. Frenzel<sup>5,6</sup> , M. A. Johnston<sup>7</sup> , M. Cornec<sup>6,8</sup> , and E. Osborne<sup>1</sup> 

<sup>1</sup>NOAA/OAR/Atlantic Oceanographic & Meteorological Laboratory, Miami, FL, USA, <sup>2</sup>Global Science & Technology, Inc., Greenbelt, MD, USA, <sup>3</sup>NOAA/NESDIS/STAR/SOCD Laboratory for Satellite Altimetry, College Park, MD, USA, <sup>4</sup>Cooperative Institute for Marine and Atmospheric Studies, Rosenstiel School for Marine, Atmospheric, and Earth Science, University of Miami, Miami, FL, USA, <sup>5</sup>Cooperative Institute for Climate, Ocean, and Ecosystem Studies, University of Washington, Seattle, WA, USA, <sup>6</sup>NOAA/OAR/Pacific Marine Environmental Laboratory, Seattle, WA, USA, <sup>7</sup>NOAA/NOS/Flower Garden Banks National Marine Sanctuary, Galveston, TX, USA, <sup>8</sup>School of Oceanography, University of Washington, Seattle, WA, USA

**Abstract** Coral reefs globally are experiencing more frequent and severe warming events due to anthropogenic driven climate change. Subtropical reefs experience more seasonal variability than lower latitude reefs making them typically more resilient to climate change. With relatively stable coral cover in comparison to other global coral reefs, Flower Garden Banks National Marine Sanctuary (FGBNMS) in the Gulf of Mexico is a series of 17 reefs and banks located on the continental shelf-edge containing a variety of shallow (0–30 m) and mesophotic (30–150 m) coral reef habitats. Here, we use satellite data products to associate open ocean Argo float profiles with eddy features over FGBNMS to study the shelf-edge reef environment spanning nearly two decades (2003–2022). Satellite data show that FGBNMS is frequently influenced (~15 days/month) by mesoscale eddies. The upper water column variability (0–25 m) is most influenced by the seasonal mixed layer despite eddy interaction. Subsurface seasonal ranges of temperature and salinity are enhanced or suppressed depending on the influence of eddies in relation to the mixed layer depth. Within the mesophotic zone (0–150 m), the largest range of thermal variability between anticyclonic and cyclonic eddies is between 50 and 150 m upwards of 5°C. However, these observed dynamics will likely change as a result of eddy variability associated with projected warming and Loop Current weakening, leading to increased thermal stress in the future.

**Plain Language Summary** Coral reefs globally are threatened by climate change, yet some reefs are less impacted than others, such as coral reef habitats in Flower Garden Banks National Marine Sanctuary (FGBNMS) located in the northwestern Gulf of Mexico. This study demonstrates an exposure to large temperature and salinity ranges across different depths throughout the year which may aid in the resiliency and longevity of this ecosystem. The Gulf of Mexico contains some of the most energetic eddies, or spinning currents, in the world. While these eddies originate in the open ocean, they are mobile features that move onto FGBNMS over the shelf-edge ~15 days/month, translating open ocean physical and biogeochemical signatures. Here we find that the eddies on FGBNMS show significant alterations to temperature and salinity conditions. Importantly, the physical oceanography driving the eddy field is expected to weaken under climate change, potentially threatening this unique shelf-edge reef system, and subjecting the coral reef habitats to warmer ocean temperatures in the future.

### 1. Introduction

Flower Garden Banks National Marine Sanctuary (FGBNMS), located on the shelf-edge in the northwestern Gulf of Mexico, consists of 17 reefs and banks with some of the healthiest coral reefs in the Caribbean region. The East Flower Garden Bank and West Flower Garden Bank have maintained >50% coral cover over the past 30 years (Johnston et al., 2016, 2021; Kealoha et al., 2020). Global coral reefs have been experiencing a rapid decline in recent years, largely attributed to anthropogenic warming of sea surface temperatures (SSTs; Eakin et al., 2010; Hughes et al., 2018; Skirving et al., 2019). Despite global declines, the coral reefs on East Flower Garden Bank and West Flower Garden Bank have been deemed one of the most persistent coral reef ecosystems in the world (Jackson et al., 2014; Johnston et al., 2016; Johnston, Hickerson, et al., 2019). Resilience in this location can

**Resources:** J. K. McWhorter, H. L. Roman-Stork, M. A. Johnston, M. Cornec, E. Osborne  
**Software:** J. K. McWhorter, H. Frenzel, M. Cornec  
**Supervision:** J. K. McWhorter, M. Le Hénaff, E. Osborne  
**Validation:** J. K. McWhorter, H. Frenzel  
**Visualization:** J. K. McWhorter, H. L. Roman-Stork  
**Writing – original draft:** J. K. McWhorter  
**Writing – review & editing:** J. K. McWhorter, H. L. Roman-Stork, M. Le Hénaff, H. Frenzel, M. A. Johnston, M. Cornec, E. Osborne

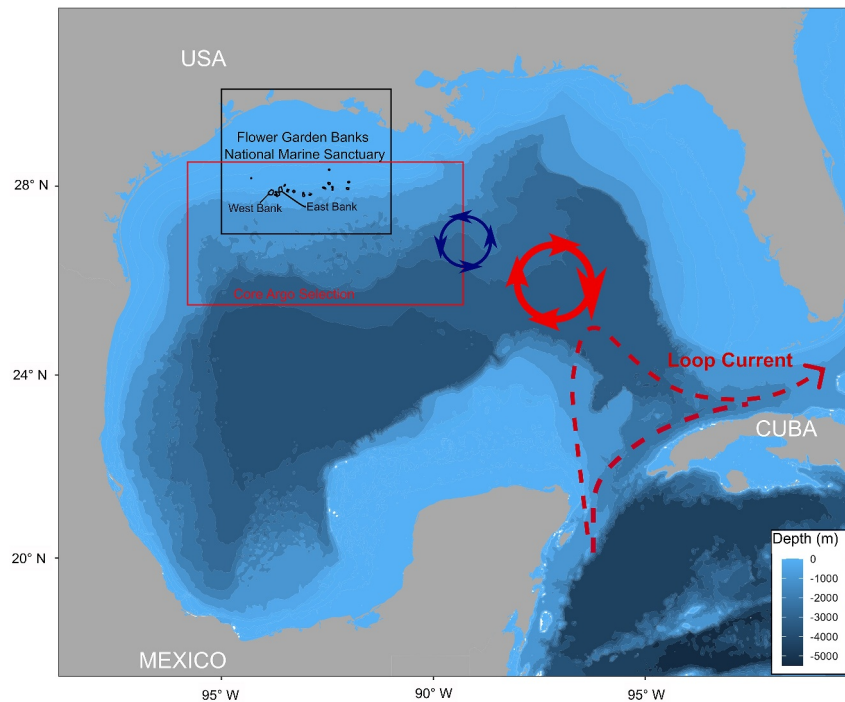


**Figure 1.** The Gulf of Mexico is shown with bathymetry shaded in blue and the 17 reefs and banks comprising Flower Garden Banks National Marine Sanctuary (FGBNMS) outlined in black. The selection for Core Argo profiles is defined by a red box. The diagram shows the Loop Current dashed in red which can expand northward and retract southward. A red circle represents an anticyclonic eddy (downwelling), and a blue circle represents a cyclonic eddy (upwelling). The grid used for the eddy analysis is the black rectangle surrounding FGBNMS (27–30°N, 91–95°W).

potentially be attributed to seasonal variability of temperatures experienced by a high latitude reef (Courtney et al., 2017; Kealoha et al., 2020; Kleypas et al., 1999), deep water (>30 m) thermal stability relative to shallow reefs (<10 m), the distance (190 km) from coastal anthropogenic stressors (i.e., nutrient runoff), oligotrophic open ocean like conditions, and the federal protections limiting anthropogenic activities within the sanctuary (Johnston et al., 2016). Temperatures on FGBNMS can range from ~20 to 30°C based on two mooring locations on East Flower Garden Bank and West Flower Garden Bank at ~20 m depth (Johnston, Hickerson, et al., 2019). Well-studied coral sites on East Flower Garden Bank and West Flower Garden Bank even showed slight increases in coral coverage from 1989 to 2014 (Johnston et al., 2016; Manzello et al., 2021).

The location of FGBNMS on the shelf-edge means that it is more readily exposed to open ocean influences (Kealoha et al., 2020; Teague et al., 2013). Therefore, open ocean physical processes are of importance to understanding the range of environmental conditions experienced, and by extension, the resiliency of this reef ecosystem. The Loop Current is by far the most dominant physical current system within the Gulf of Mexico, and has a significant influence on the biogeochemistry of the water masses it influences (Xu et al., 2019). The Loop Current enters the Gulf of Mexico near the Yucatan Peninsula and delivers warm, saline waters from the Caribbean Sea to predominantly the eastern Gulf of Mexico, regulating the influence of the Atlantic basin on the region (Brokaw et al., 2020; Sturges & Evans, 1983) (Figure 1). The Loop Current exits around the Florida Straits where it then directly feeds into the Gulf Stream. Within the Gulf of Mexico basin, the Loop Current extends and retracts north to south across the entire deep basin on variable time-scales and often sheds large, westward moving anticyclonic (downwelling) warm water eddies. These eddies are often referred to as Loop Current Rings. In contrast, vorticity perturbations along the Loop Current lead to the formation of cyclonic (upwelling) cold water eddies that are often involved in the pinching of the Loop Current or the detachment of anticyclonic eddies (Brokaw et al., 2020; Le Hénaff et al., 2014; Zavala-Hidalgo et al., 2003). Cyclonic eddies can also form along a Loop Current Ring inside the Gulf of Mexico when encountering steep bathymetry near the Mexican shelf-edge (Hamilton et al., 2002). Whereas most of the Gulf of Mexico is characterized by Gulf Common Waters, or waters with a maximum subsurface salinity of 36.3–36.4 PSU between 125 and 250 m (de Lanza Espino et al., 2004).

The Loop Current and the associated Loop Current Rings carry warm waters from the Caribbean Sea, with a deeper thermocline and a salinity maximum in the subsurface (100–300 m) characteristic of the Subtropical Underwater (Gordon, 1967).

Mesoscale eddies trap and transport heat, salt, nutrients, and other physical and biogeochemical characteristics throughout the ocean (Brokaw et al., 2020; Chaigneau et al., 2009; Chelton et al., 2011; Moreau et al., 2017; Patel et al., 2020; Strutton et al., 2023) through a process known as eddy pumping, or thermocline changes between anticyclonic and cyclonic eddies (Falkowski et al., 1991; McGillicuddy Jr, 2016; McGillicuddy Jr et al., 1998; Siegel et al., 1999; Strutton et al., 2023). Eddy pumping results in increases of surface layer nutrients in cyclonic eddies and decreases of nutrients in anticyclonic eddies (Dawson et al., 2018; Siegel et al., 2011; Strutton et al., 2023). Eddies can have important ecosystem functions for reef habitats such as transporting larvae (Domingues et al., 2016; Limer et al., 2020; Lugo-Fernández et al., 2001; Teague et al., 2013), distributing nutrients, and potentially providing thermal reprieve or driving additional thermal (Wyatt et al., 2023) and biogeochemical stress (Kealoha et al., 2020). The eddy field surrounding FGBNMS has yet to be quantified in a continuous, multi-decadal framework, informed by water column properties of temperature and salinity. Since the Loop Current is a large driver of the eddy field in the Gulf of Mexico, a projected weakening of the Loop Current under climate change (Liu et al., 2015) could alter the eddy conditions that pass over shelf-edge reef ecosystems.

Here we use a combination of observational time series to expand our knowledge from surface satellite information into the depth dimension. Core Argo floats, which are autonomous ocean profiling floats (collecting data from 0 to 2,000 m), were first deployed to collect data in the Gulf of Mexico in 2003 and the program rapidly increased in 2010. These Lagrangian platforms often come into contact with Loop Current Rings (anticyclonic eddies) as well as cyclonic eddies. In this study, Core Argo floats provide a continuous, long-term dataset on subsurface temperature and salinity used to investigate the interaction of eddies with FGBNMS. In addition to the interaction of eddies, the mixed layer, or the homogenous temperature, salinity and density that form as a result of upper layer turbulent mixing, provides important context of upper layer conditions that may be transferred to the reef environment depending on temporal and spatial variability (Brainerd & Gregg, 1995; de Boyer Montégut et al., 2004; Kara et al., 2003).

## 2. Data and Methods

### 2.1. Study Area

FGBNMS is the only national marine sanctuary in the Gulf of Mexico, located 50 to 77 miles (80–123 km) off the coasts of Texas and Louisiana and ranging in depth from 16 to 220 m. FGBNMS consists of a combination of 17 reefs and banks perched atop underlying salt domes along the continental shelf forming a chain of protected habitats including thriving shallow water coral reefs, algal-sponge communities, and mesophotic reefs comprised of black coral, octocoral, and algal nodule habitats (Etnoyer et al., 2021; Rezak et al., 1985). The original three banks of FGBNMS included East Flower Garden Bank, West Flower Garden Bank, and Stetson Bank, and 14 more banks were added in 2021, including Horseshoe, MacNeil, Rankin, 28 Fathom, Bright, Geyer, Elvers, McGrail, Bouma, Sonnier, Rezak, Sidner, Parker, and Alderdice Banks (86 Fed. Reg. 4937 [19 Jan 2021]). The study area for this paper includes all 17 reefs and banks of FGBNMS. The depth range of 0–150 m was selected for analysis as East and West Flower Garden Banks span from 14 to 150 m containing the most well-studied and most dense coral cover in the sanctuary (Johnston et al., 2016; Johnston, Hickerson, et al., 2019; Johnston, Nuttall, et al., 2019).

### 2.2. Core Argo Array

Core Argo floats, which are autonomous open ocean profiling floats (collecting data from 0 to 2,000 m), were first deployed to collect data in the Gulf of Mexico in 2003 and then expanded largely in 2010 (Figure S1 in Supporting Information S1). These Lagrangian open ocean profiling floats measure temperature, salinity, and depth. Generally, Argo floats collect a 2,000 m profile once every 10 days. Data from the international Argo program can be accessed from one of two identical global data assembly centers and are available in near-real time (see data availability section (Argo, 2020)) (A. P. Wong et al., 2020).

The OneArgo-R toolbox (Cornec et al., 2022) and the “argodata” package in R (Kelley et al., 2021) were used for the Core Argo float selection process. Core Argo floats were selected based on location in the western Gulf of

Mexico (28.5–25.5°N, 95.8–89.3°W) and filtered to select delayed mode (D mode) temperature and salinity data with a quality control flag of 1 ( $n = 1,710$ , 2003–2022) (A. Wong et al., 2022; A. P. Wong et al., 2020). The Mixed Layer Depth (MLD) was calculated using a density threshold method (de Boyer Montégut et al., 2004; Holte & Talley, 2009) that used float temperature and salinity data in the OneArgo-R toolbox (Cornec et al., 2022). This method examines deeper levels of density until a depth level is found that is  $0.03 \text{ kg m}^{-3}$  greater than the 10 m reference depth value (de Boyer Montégut et al., 2004).

Argo float measurements are not taken at fixed depths; therefore, a depth interpolation was used to create a standardized grid using 0.2 m intervals from 0 to 2,000 m with a linear interpolation across variables (See data availability section for code details). A linear interpolation was then used between observed temperature levels (Suga et al., 2004) to extract the depth that best falls under the difference criteria (Cornec et al., 2022; de Boyer Montégut et al., 2004; Frenzel et al., 2022). The means and standard deviations were then taken within each depth for temperature and salinity by month and eddy type (anticyclonic eddy, cyclonic eddy, and no eddy) across the timeseries.

The Core Argo float hydrographic profiles and associated mixed layer were then associated with an eddy type; anticyclonic eddy, cyclonic eddy, or no eddy using the adapted multiparameter mesoscale eddy tracking method discussed in Sections 2.3 and 2.4 (Roman-Stork et al., 2023). Across the entire Gulf of Mexico domain, on average there were 42 ( $\pm 11$ ) anticyclonic eddy profiles, 43 ( $\pm 9$ ) cyclonic eddy profiles, and 57 ( $\pm 14$ ) no eddy profiles for each month from 2003 to 2022 within 28.5–25.5°N, 95.8–89.3°W (Figure S1 in Supporting Information S1).

Data from 0 to 150 m were prioritized for analysis to emphasize the hydrographic data directly associated with “shallow” corals (14–30 m) and mesophotic (30–150 m) coral reef communities found on FGBNMS.

### 2.3. Satellite Data

The version of eddy tracking used in this study (Section 2.4) is based entirely on gridded satellite data products. For the purposes of this study, eddy fields were based on Copernicus Marine Environmental Monitoring Service (CMEMS) sea level anomalies (SLA) and geostrophic currents (Ducet et al., 2000; Le Traon et al., 1998; Taburet et al., 2019), which are a level 4 data product derived from the 1993–2012 mean and processed with the Data Unification and Altimeter Combination System (DUACS) multimission altimeter processing system. This product has a spatial resolution of  $0.25^\circ \times 0.25^\circ$  and was obtained with daily temporal resolution from 1 September 2002 through 31 July 2022.

National Oceanographic and Atmospheric Administration (NOAA) geo-polar daily night SST data (Maturi et al., 2017) were also incorporated into the eddy tracking system and were tracked along with characteristics and trajectories, but these data were not involved in the calculation of either trajectories or contours. Geo-polar blended SST is a level 4 daily product available from NOAA Coast Watch at 5 km horizontal resolution, and was obtained from 1 September 2002 through 31 July 2022 given the dataset's start date of 1 September 2002.

### 2.4. Multiparameter Mesoscale Eddy Tracking

The eddy field surrounding FGBNMS was compared to the surrounding Gulf of Mexico using the MULTiparameter Near real time System for Tracking Eddies Retroactively (MUNSTER). MUNSTER, in development at NOAA's Laboratory for Satellite Altimetry, uses a closed contour eddy tracking methodology based on NOAA Radar Altimeter Database System (RADS) SLA and geostrophic currents (Chaigneau et al., 2008, 2009; Pegliasco et al., 2015; Roman-Stork et al., 2023; Scharroo et al., 2013). This method also tracks additional multiparameter variables, that is, SST, sea surface salinity, and ocean color chlorophyll-a. An earlier version of this method has been reliably used in the Indian Ocean (Greaser et al., 2020; Roman-Stork et al., 2019; Trott et al., 2019), the western North Atlantic (Roman-Stork et al., 2023), and the Gulf of Mexico (Brokaw et al., 2020; Roman-Stork et al., 2023) to analyze mesoscale eddy variability and air-sea interactions.

For the analysis performed in this study, a modified extended version of MUNSTER (Roman-Stork et al., 2023) was used based on the CMEMS SLA fields rather than the NOAA RADS fields (Ducet et al., 2000; Le Traon et al., 1998). Error estimates can therefore be derived from altimetry and the closed-contours (Chaigneau et al., 2008, 2009; Ducet et al., 2000; Le Traon et al., 1998; Pegliasco et al., 2015; Taburet et al., 2019). Gaussian filtering for planetary waves was also performed with a  $10^\circ$  longitude,  $20^\circ$  latitude semi-width high pass filter



similar to those used in other eddy tracking systems (Chelton et al., 2011; Mason et al., 2014). MUNSTER is threshold free in both time and space, which allows for the tracking of more transient (short lived, low amplitude) eddies. While this does result in some false eddies and filaments being included, transient eddies can play a significant role in air-sea interactions (Roman-Stork et al., 2019) and storm development (Greaser et al., 2020), as well as the upper ocean circulation (Roman-Stork et al., 2023), and should not be disqualified when considering the full ocean circulation.

MUNSTER produces eddy contours, characteristics, and trajectories, where values are tracked based on the eddy centroid. Trajectories are calculated using a cost function (CF) based on eddy kinetic energy (EKE), eddy radius ( $R$ ), and eddy amplitude ( $A$ ):

$$CF_{e_1, e_2} = \sqrt{\left(\frac{\Delta R - \overline{\Delta R}}{\sigma_{\Delta R}}\right)^2 + \left(\frac{\Delta A - \overline{\Delta A}}{\sigma_{\Delta A}}\right)^2 + \left(\frac{\Delta EKE - \overline{\Delta EKE}}{\sigma_{\Delta EKE}}\right)^2} \quad (1)$$

where  $e_1$  and  $e_2$  are the eddy's placement in between time steps,  $\Delta$  represents the difference between points,  $\sigma$  is the standard deviation, and a bar above a variable indicates a mean. Eddy trajectories are considered valid if the algorithm is run for a period longer than 100 days.

Given the goal of creating a 20-year climatology, sea surface salinity and ocean color chlorophyll- $a$  grids that do not span this temporal frame were omitted from the tracked variables, such that only SST was included from the multiparameter analysis along with altimetry-derived quantities, such as EKE, relative vorticity, divergence, and the Okubo-Weiss parameter. Due to data availability limitations (i.e., available date ranges of data sets used at the time of writing), eddy tracking was run from 1 September 2002 through 31 July 2022 in the Gulf of Mexico.

The area surrounding FGBNMS (27–30°N, 91–95°W) was compared to the entire Gulf of Mexico (15–30°N, 80–100°W) to determine the EKE relative to Loop Current extension conditions, and obtain other spatial statistics relative to the eddies (Figure S3 in Supporting Information S1). The area surrounding FGBNMS was then used to quantify the monthly frequency of anticyclonic eddy and cyclonic eddy days over FGBNMS. MUNSTER was then used to geographically associate Core Argo float profiles with eddies in the Gulf of Mexico from 2003 to 2022. The spatial extent was limited to the western Gulf of Mexico (17–30°N, 88.1–100°W) to provide water column data closer to FGBNMS (Figure 1).

### 3. Results

In the FGBNMS region (Figure 1), there is a high presence of eddies (Figures 2 and 3) driving enhanced changes in temperature and salinity (Figures 4–8) on top of the seasonal variability of the upper mixed layer (Figure 5a). Broadly, across the Gulf of Mexico the MLD is generally deeper during wintertime when surface winds are stronger resulting in mixing over the upper water column, with the opposite occurring during summertime months (Figure 5a). The location of the average MLD ranges from 50 m in February and 25 m in July (Figure 5a, Figure S2 in Supporting Information S1), seasonally exposing different water column characteristics over various depths on the reef. Eddy pumping shows differences between eddy types of more than 5°C during late summer/early fall (Aug–Oct) between 50 and 150 m (Figure 7a). It has been noted that eddy pumping can result in extreme conditions over a coral reef environment, such as an anticyclonic eddy enhancing temperatures (Wyatt et al., 2023), although we did not find a direct correlation between eddy pumping and FGBNMS coral stress (Figure 4, Figures S4 and S5 in Supporting Information S1).

Twenty years of eddy trajectories in the Gulf of Mexico filtered by EKE thresholds and eddy type describe the generalized eddy energetics of the region (Figures 2g–2j). Lower energy eddies ( $<500 \text{ cm}^2/\text{s}^2$ ) are typically found outside of the Loop Current Extension, especially in the western Gulf of Mexico, and dominate the region of FGBNMS. Of the fewer, more energetic eddies that pass over FGBNMS (Figures 2e–2d), most are anticyclonic, with several being Loop Current Rings but in general, the most energetic eddies (Figures 2a and 2b), with rare exception, do not travel near FGBNMS. In calculating the mean EKE for the area around FGBNMS (27–30°N, 91–95°W) compared with the overall Gulf of Mexico (17–30°N, 80–100°W), over the twenty-year period, eddies around FGBNMS were on average 78% less energetic. Mean cyclonic eddies in FGBNMS contain a value of  $112 \text{ cm}^2/\text{s}^2$  compared to  $487 \text{ cm}^2/\text{s}^2$  in the overall Gulf of Mexico and FGBNMS anticyclonic eddies having a value of  $100 \text{ cm}^2/\text{s}^2$  compared to  $458 \text{ cm}^2/\text{s}^2$  in the overall Gulf of Mexico (Figure 2).

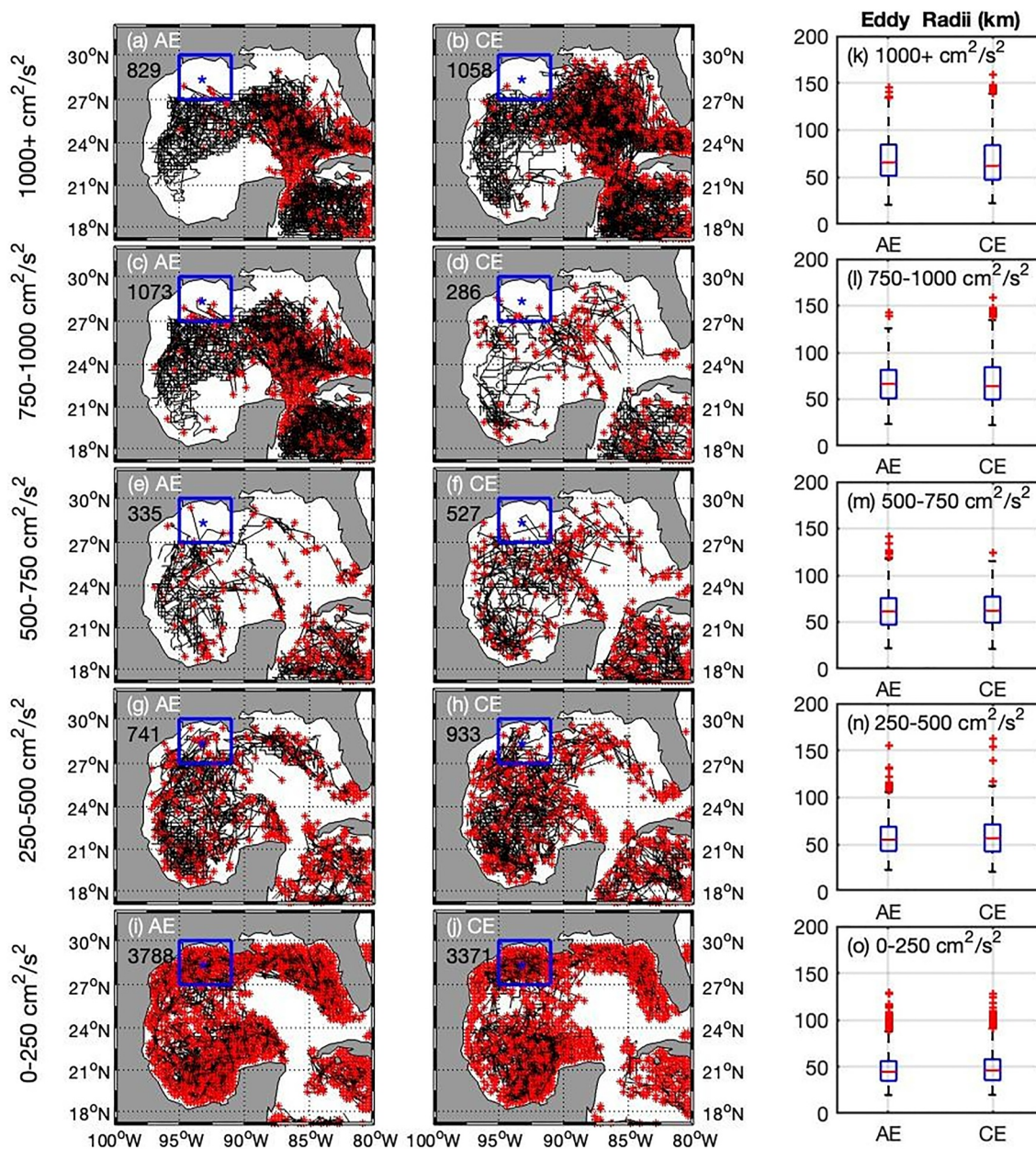


**Figure 2.** Anticyclonic eddy (AE) and cyclonic eddy (CE) trajectories in the Gulf of Mexico (15–30°N, 80–100°W) categorized by eddy kinetic energy (a–j) and radii (km; k–o) from September 2002 to July 2022 using the modified multiparameter eddy tracking system. Red stars indicate the location of eddy generation, black lines are eddy trajectories, and numbers in black indicate the number of eddies per plot. The blue stars indicate the location of the Flower Garden Banks National Marine Sanctuary and the boxes surrounding them indicate the region used for time series analysis. (27–30°N, 91–95°W).

Eddies are present in the FGBNMS region on average for more than half of the days in each month (Figure 3). Cyclonic eddies are most frequent March–May and September, with the peak occurring in May, of 22 average eddy days/month (Figure 3). Consistent with Limer et al. (2020), the peak frequency in anticyclonic eddy days occurs in May–July and November–December (study design; 2004–2018, 25 km box around the sanctuary), although our results show the peak of 17 days as opposed to 10 days. While a reflection of the natural variability, the high range of eddy monthly frequency is also driven by the years chosen, area specified, and the eddy detection method.

Seasonal temperature variability is modulated through eddy pumping (Figures 5a and 5b) influencing the conditions over the reef (Figures 6–8). Core Argo float profiles from the western Gulf of Mexico (28.5–25.5°N, 95.8–

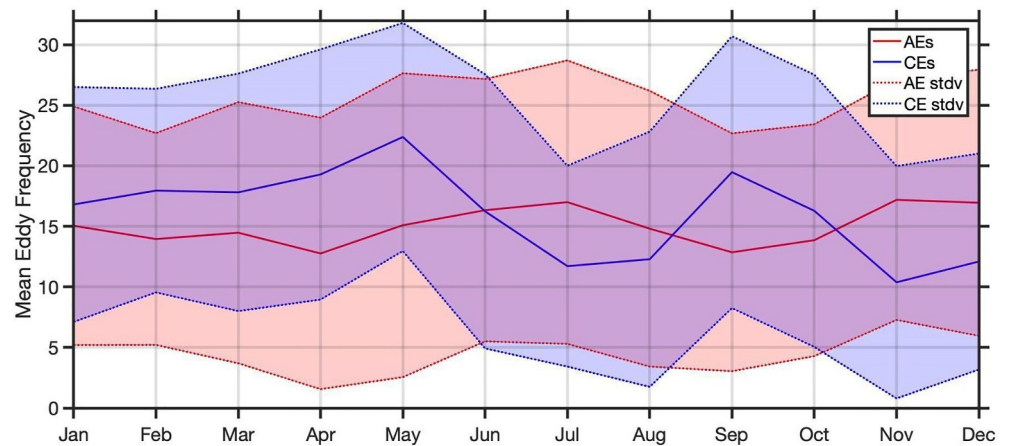


**Figure 3.** Seasonal cycles of eddy frequency (mean eddy days per month) in the Flower Garden Banks National Marine Sanctuary region (27–30°N, 91–95°W) from September 2002 to July 2022 for anticyclonic eddies (AEs; red; downwelling) and cyclonic eddies (CEs; blue; upwelling). Dotted lines and shaded regions indicate  $\pm 1$  standard deviation for AEs (AE stdv; red) and CEs (CE stdv; blue).

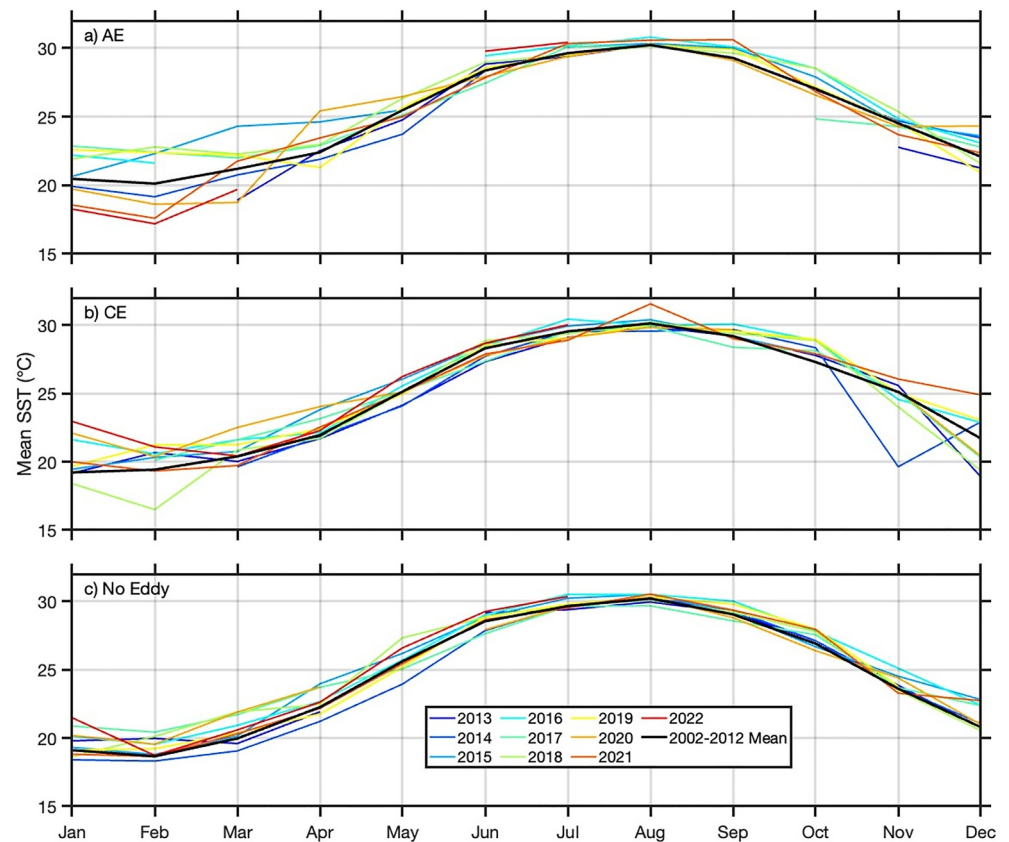


**Figure 4.** Time series of monthly mean SST (°C) in the Flower Garden Banks National Marine Sanctuary region (27–30°N, 91–95°W) in anticyclonic eddies (AE; a), cyclonic eddies (CE; b), and when no eddy is present (No Eddy; c), organized by year and compared to the 2002–2012 mean, which varies between eddy type. No significant coral bleaching events occurred from 2013 to 2022 other than the hypoxic event in 2016 and a coral disease event in 2022, which were coupled with anomalously warm SSTs.



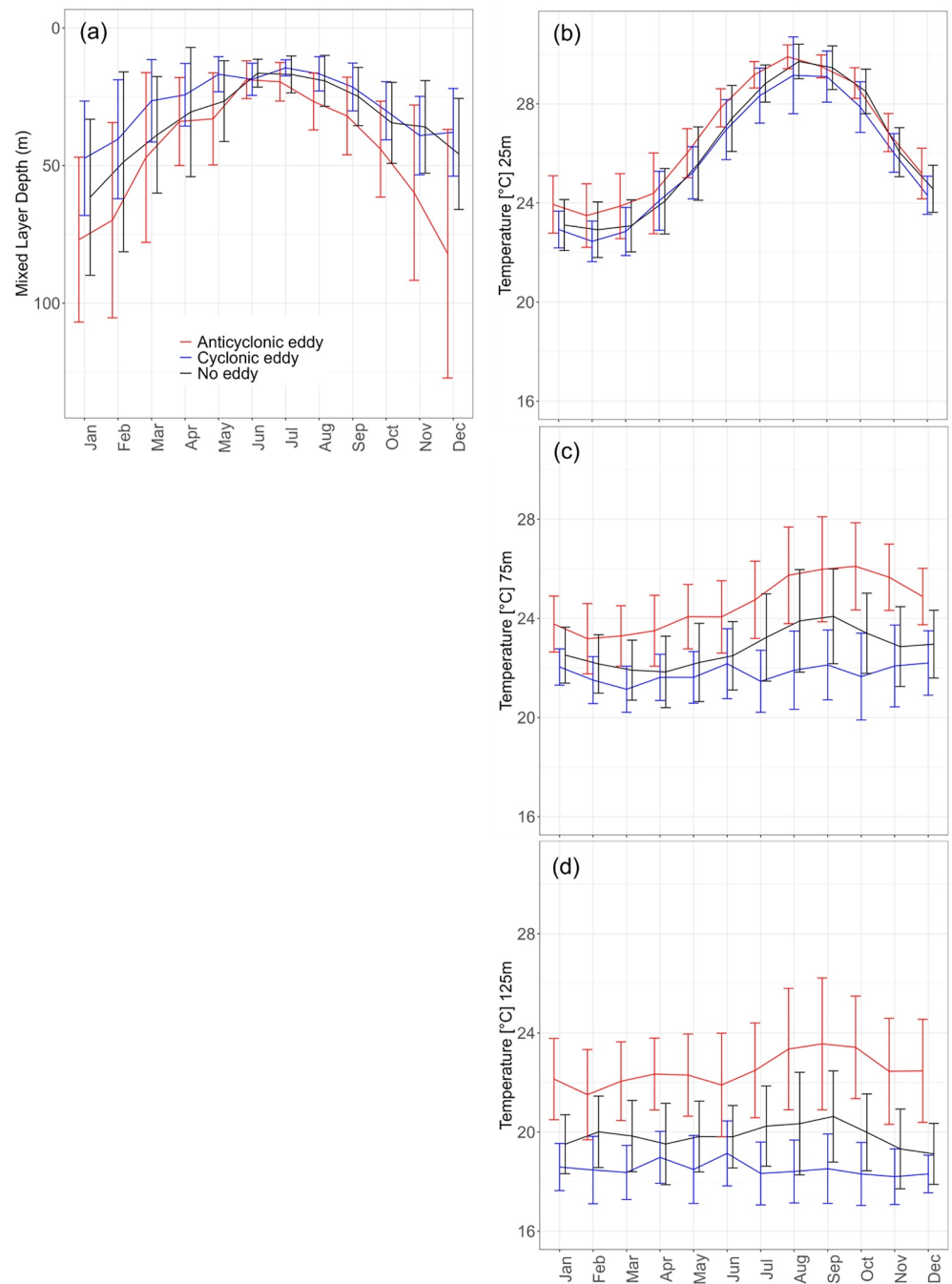


**Figure 5.** (a) Mixed Layer Depth, and temperature variability at (b) 25 m, (c) 75 m, and (d) 125 m are shown using monthly averages and standard deviations from Core Argo float profile density data categorized by anticyclonic eddies (red), cyclonic eddies (blue), or no eddy (black) from 2003 to 2022 in the western Gulf of Mexico (28.5–25.5°N, 95.8–89.3°W).

89.3°W) adjacent to FGBNMS from 2003 to 2022 were aggregated to demonstrate that MLDs generally shoal in summer months and deepen in winter months (Figure 5a). As eddies near the reef environment, vertical transport driven by eddy-pumping can move the warm surface waters deeper (anticyclonic downwelling) or cooler deeper waters to shallower water column depths (cyclonic upwelling) (Figures 5–8). Compared to the baseline state (i.e., or no eddy conditions) on average anticyclonic eddies increase temperatures while cyclonic eddies decrease temperatures (Figures 5c and 5d, and 6). As marine heatwaves are event driven, the frequency of both eddy types based on timing could provide additional coral reef stress or reprieve.



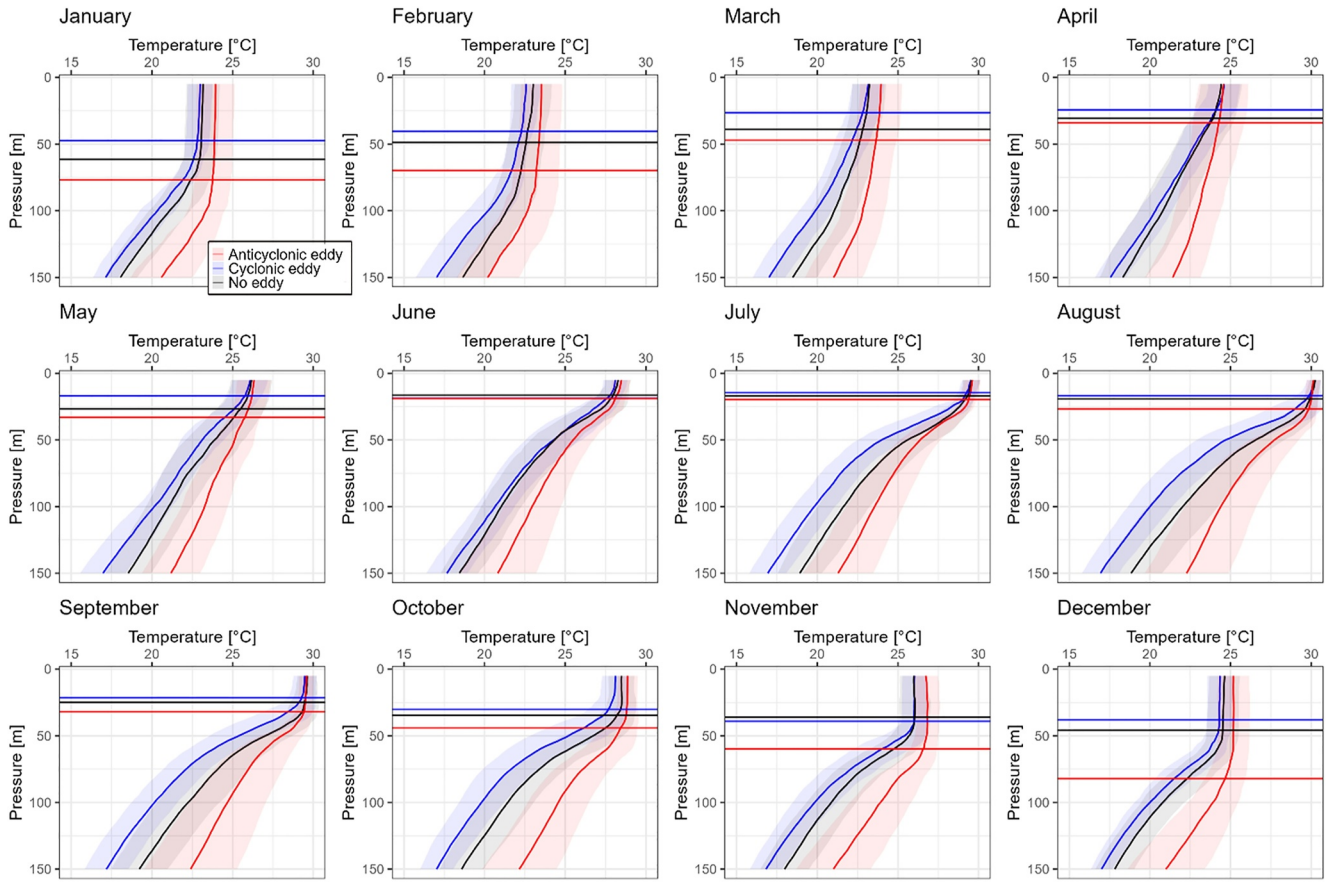


**Figure 6.** The mean temperatures from Core Argo floats in the Gulf of Mexico (28.5–25.5°N, 95.8–89.3°W) are associated with cyclonic eddies (CE, blue), anticyclonic eddies (AE, red), or no eddy (NE, black) from 2003 to 2022 by month. The shaded areas represent standard deviations. Mixed layer depth using density criteria is shown on average with the horizontal lines within cyclonic eddies (CE, blue), anticyclonic eddies (AE, red), or no eddy (NE, black). Depth was intentionally limited to the upper water column for mesophotic reef context (0–150 m).

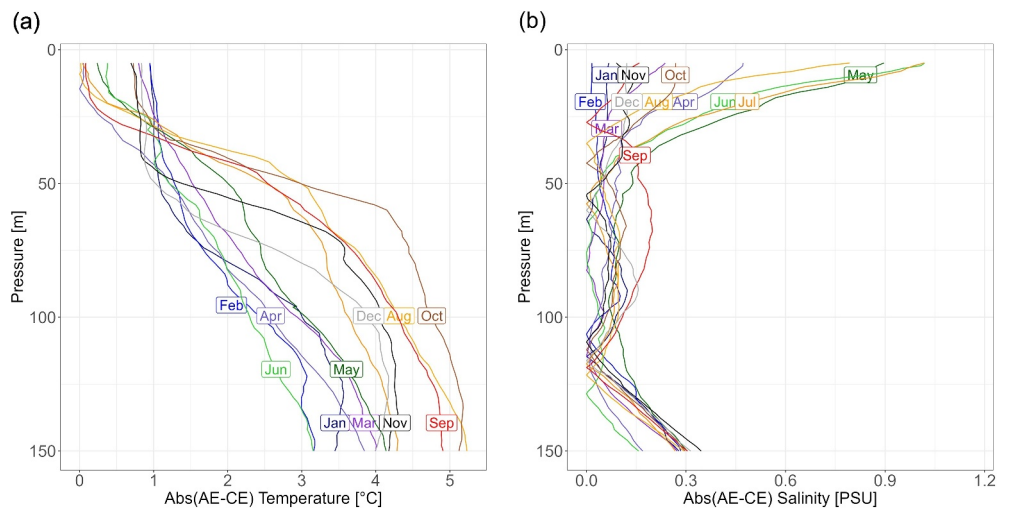


**Figure 7.** The absolute differences between anticyclonic (AE) and cyclonic eddy (CE) profiles were taken across depths 0–150 m per month for (a) temperature and (b) salinity (28.5–25.5°N, 95.8–89.3°W).

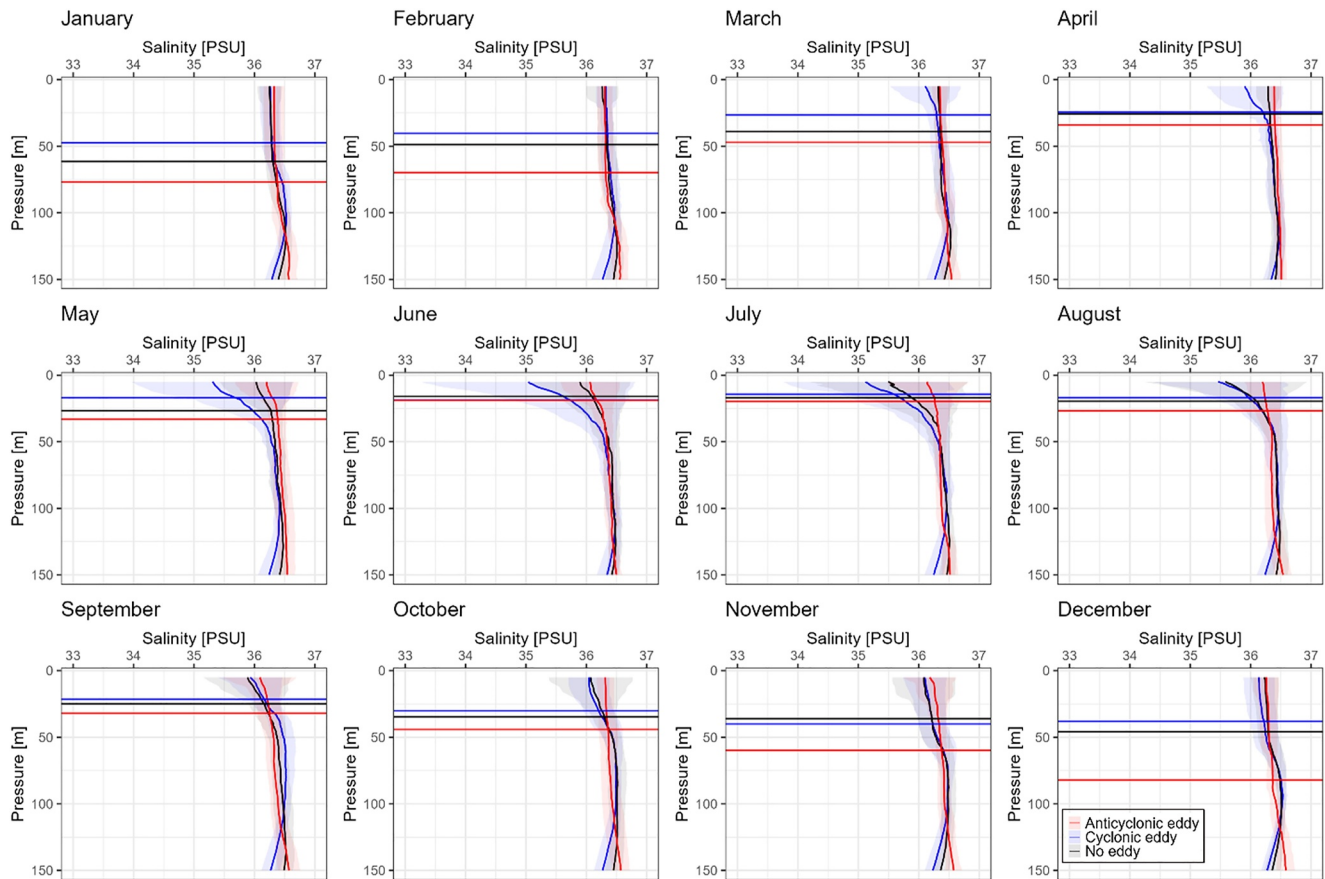


**Figure 8.** The mean salinity values from Core Argo floats in the Gulf of Mexico (28.5–25.5°N, 95.8–89.3°W) are associated with cyclonic eddies (CE, blue), anticyclonic eddies (AE, red), or no eddy (NE, black) from 2003 to 2022 by month. The shaded areas represent standard deviation. Mixed layer depth using density criteria is shown on average with the horizontal lines within cyclonic eddies (CE, blue), anticyclonic eddies (AE, red), or no eddy (NE, black). Depth was intentionally limited to the upper water column (0–150 m).

Anticyclonic eddies in the winter generally enhance the depth of the mixed layer by an additional 25–30 m from waters with no eddies and cyclonic eddies (Nov, Jan, Feb,  $p$ -value < 0.05 (depth < 150 m)) (Figure 5; Table S1 in Supporting Information S1). Cyclonic eddies generally shoal the MLD, although during summer months when MLD is seasonally shallow, cyclonic eddies appear to have a negligible influence on further shoaling MLD (average ~22 m) (Figure 5; Table S1 in Supporting Information S1). Temperature variability in the upper water column (<25 m) is dominated by the seasonal MLD change (Figures 5a and 5b) in comparison to the increased range of temperature driven by anticyclonic and cyclonic eddies at 125 m (Figures 5b and 5d). The thermal variability at 75 m can be described as a transition zone where a combination of the seasonal surface-derived signal is mixed with the physical eddy-associated signal (Figure 5c). The seasonal mixed layer at 75 m is apparent since during winter months, when the MLD is deepest, the temperatures are more similar across eddy types while in summer months, when MLD is shoaled, eddy types show more distinct temperatures demonstrating the physical eddy-associated signal (Figure 5c).

FGBNMS coral reef stress due to anomalously warm temperatures, while minimal in comparison to global coral reefs, has typically occurred during the months of August–September (Johnston, Hickerson, et al., 2019; Johnston, Nuttall, et al., 2019). SSTs during the month of August reveal warm temperatures commonly exceeding 30°C above the mixed layer across all three water masses (anticyclonic, cyclonic, no eddy; Figures 4 and 6). Importantly, the vertical transport within an anticyclonic eddy will downwell these warm surface waters, increasing the depth range of potential thermal stress on the coral reef, and conversely a cyclonic eddy will upwell deep, cooler waters potentially alleviating top-down thermal stress. Our analysis shows an August temperature range from 30°C at the surface across eddy types to as much as 18°C at 150 m associated with monthly average cyclonic eddy conditions (Figure 6). Differences in temperature between anticyclonic and cyclonic eddies are greatest below the

mixed layer (Figures 5b–5d, 6, and 7a). Temperature differences between anticyclonic and cyclonic eddies are on average 5°C between 50 and 150 m from August to December (Figures 5c and 5d, 6, and 7a). Above the mixed layer anticyclonic eddies show the largest difference compared to other water masses with warmer temperatures on the order of 1–2°C greater from October to April (Figures 5b and 6).

During years of recorded coral stress on East Flower Garden Bank and West Flower Garden Bank within our time series (2005 (warming), 2010 (warming), 2016 (dominant hypoxic conditions), 2022 (coral disease)), typically seen August–November, anticyclonic and cyclonic eddies both contained anomalously warm SSTs (>30°C, Figure 4). This indicates that the entire Gulf of Mexico was anomalously warm and warming was not additionally driven by an anticyclonic eddy or a warm water mass. EKE values during coral stress years (Figure 4) show no pattern of deviation from the mean, suggesting that Loop Current Rings or other highly energetic eddies did not directly force previous stress events in this region.

In order to determine if later years were warming more than early years, satellite SST data were used for the comparison. Early years (2002–2012) were used to derive a climatology and later years (2013–2022) were used annually. While summer SSTs generally increased from early to later years, the summer SSTs did not vary between eddy types (anticyclonic, cyclonic, and no eddy) (Figure 4). This suggests that the entire region surrounding FGBNMS was warm on the surface during summer, regardless of eddy type. No significant coral bleaching events occurred from 2013 to 2022 other than the hypoxic event in 2016 and a coral disease event in 2022, which were both coupled with anomalously warm SSTs (Johnston, Hickerson, et al., 2019; Johnston, Nuttall, et al., 2019; Johnston et al., 2023).

During winter and spring months (Nov–Apr), we observe an increase in the SST range in the presence of eddies compared with no eddy conditions in recent years (2013–2022) (Figure 4) relative to the climatology (2002–2012). Anticyclonic eddies show large winter temperature variations above and below the climatological mean (Figure 4). In cyclonic eddies during winter months, all but two recent year's temperatures (2013, 2018) were above the 2002–2012 mean, suggesting a subsurface warming signal (Figure 4). As the Core Argo profiles do not have a strong distribution of data from 2002 to 2012 we could not use these data to detect a complementary climate signal to satellite observations (Figures S1b and S6, Table S2 in Supporting Information S1). However, a recent Gulf of Mexico analysis (1993–2017) indicated significant subsurface warming across the region below ~200 m (Steinberg et al., 2024, p. 2) and we anticipate that the climate signal will increase overtime due to warming trends and the growing Argo array.

Salinity values above the mixed layer range on average from 34 to 37 PSU in summer months (May–August), reflecting the largest range of salinity throughout the year (Figures 7b and 8). Cyclonic eddies show the largest difference in salinity from the surface to depth from April to August (Figure 8) as surface freshening due to seasonal rainfall/riverine inputs in combination with the more saline waters being brought up toward the surface through upwelling. Salinity values are slightly greater in cyclonic eddies between depths of 50–100 m in comparison to anticyclonic eddies and no eddy waters (Figure 8).

## 4. Discussion

### 4.1. Eddy Dynamics

Eddy characteristics in the Gulf of Mexico are generally dominated by ocean bathymetry and the location of the Loop Current (Le Hénaff et al., 2014). Compared with the overall Gulf of Mexico, FGBNMS has frequent low amplitude, low radius eddies that are topographically generated near the shelf-edge (Figure 2). Potentially providing thermal relief, cyclonic eddies contain the highest EKE variability in August–November, when the mixed layer is in the process of deepening from summer conditions (Figure 5, Figure S4 in Supporting Information S1) and the reef could be more exposed to warmer waters (Johnston et al., 2016; Johnston, Hickerson, et al., 2019; Johnston, Nuttall, et al., 2019). By contrast, the anticyclonic eddies show the largest EKE variability, with the maximum values over 1,000 cm<sup>2</sup>/s<sup>2</sup> higher than the highest cyclonic eddy values, as well as the largest variability earlier in the year, with February–May boasting the largest EKE variability for anticyclonic eddies.

### 4.2. Seasonal and Vertical Water Mass Variability

The large range of seasonal variability (surface range, 22–31°C) (Figures 5 and 6) over FGBNMS is further enhanced by frequent, low energy cyclonic and anticyclonic eddies (Figures 2 and 3). High seasonal variability is

dominantly seen above the mixed layer (0–25 m) and also within the seasonal mixed layer (25–100 m) (Figures 5 and 6). It is within the seasonal mixed layer (25–100 m) and below the seasonal mixed layer (100–150 m) where eddies increase the range of thermal variability (Figures 5 and 7a).

MLD dynamics and the presence of eddies can prevent harmful water masses from reaching coral reefs. The temperature and salinity changes over FGBNMS due to eddy conditions show a great deal of variability throughout the year contributing to coral reef resilience when exposed to extreme conditions. Anomalous SSTs typically occur in late summer months (Johnston, Nuttall, et al., 2019) therefore mixing dynamics into Aug–Nov could be important for this reef ecosystem. In the summer the lower salinity and warmer surface waters (Figures 6–8) could be prevented from reaching the deeper reefs (>30 m) due to the shallow nature of the mixed layer (Figure 5a). There are large differences between water masses above and below the mixed layer especially in summer months (Figures 5–8). Alternatively, in winter, a deeper mixed layer, even further enhanced by an anticyclonic eddy (Figure 5), could be providing necessary warm surface water temperatures down to the reef during cooler winter months since corals can also be sensitive to colder than average temperatures (González-Espinosa & Donner, 2020). Even if eddies are not directly over the reef, these water masses can influence water conditions. Teague et al. (2013) found that cyclonic eddies reversed the generally eastward current along East Flower Garden Bank in the upper water column during several days to weeks of their year-long study.

#### 4.3. Specific Events

Coral bleaching observations have been seen previously (1990, 1995, 2005, 2010, 2016 (hypoxic event), 2022 (coral disease)) during the months of August, September, October and November (Johnston et al., 2016; Johnston, Hickerson, et al., 2019; Johnston, Nuttall, et al., 2019). These events did not result in significant mortality or overall decline in coral cover (Johnston, Nuttall, et al., 2019). While a recent study in Tahiti has correlated a warm (anticyclonic) eddy to a coral bleaching event (Wyatt et al., 2023), we did not find a direct connection between an eddy event and a coral stress event (Figure 4, Figures S4 and S5 in Supporting Information S1). The largest monitored bleaching event was in summer of 2016, with 67% of East Flower Garden Bank monitored sites and 25% of sites on West Flower Garden Bank having signs of bleaching (14–30 m) (Johnston, Hickerson, et al., 2019). One study suspects the 2016 FGBNMS coral bleaching event was due to a brine release from the salt domes underneath the reef (Bright & Gittings, 2023). Alternatively, the mortality event in 2016 was found to be driven by hypoxia from river inputs (Le Hénaff et al., 2019) in combination with upwelling conditions (Kealoha et al., 2020). Coral bleaching followed the hypoxic event 10 weeks later in September 2016 (Johnston, Hickerson, et al., 2019; Kealoha et al., 2020). Hypoxia can increase bleaching susceptibility (Altieri et al., 2017; Johnson et al., 2021).

Most recently, suspected coral disease at East Flower Garden Bank and West Flower Garden Bank was reported in August 2022 associated with seven coral species that demonstrated lesions (Johnston et al., 2023). The introduction of coral disease can potentially be attributed to tissue contact through other organisms and the unique chemistry in the water column (Aeby et al., 2019; Cróquer et al., 2021; Johnston et al., 2023; Muller et al., 2020). Water quality measurements over East Flower Garden Bank and West Flower Garden Bank in 2022 did not appear to show any anomalous conditions other than slightly below average salinity but within the seasonal range (31–38 PSU) and slightly above average summer water temperature (30°C), which may have contributed to the disease spread (Johnston et al., 2023).

#### 4.4. Perspectives

Physical dynamics including eddy influence and alteration to MLD influences biogeochemistry that can be significant to reef environments (i.e., cyclonic eddies enhancing nutrient availability through eddy pumping stimulating primary production in the upper water column) (Falkowski et al., 1991; Kealoha et al., 2020; McGillicuddy Jr, 2016; McGillicuddy Jr et al., 1998; Siegel et al., 1999; Spring & Williams, 2023). The increase in Biogeochemical-Argo (BGC-Argo) floats, launched in the Gulf of Mexico in late 2021, can provide a better understanding of the chemistry and trophic conditions of the water masses within the eddies through the measurement of oxygen, nitrate, chlorophyll-a, pH, and particulate backscatter that pass over FGBNMS. The range of variability between the BGC parameters could be insightful for reef resilience as corals are mixotrophs, relying on nutrients from upwelling and particles in the water column for food as well as sunlight (Spring & Williams, 2023), and ocean acidification is a large threat to these calcifying organisms (Hoegh-Guldberg et al., 2007).



The Argo array (Core and BGC-Argo) captures eddy properties in the open ocean and satellite data can be used to attempt to fill in data gaps using eddies as the physical oceanographic conduit. Given the rapid changes occurring as a result of climate change, baseline biophysical interactions are needed to fully understand the impact of various climate change effects on our planet's resources and ecosystems. The eddy conditions around FGBNMS are important to consider as the projected weakening of the Loop Current due to anthropogenic driven climate change (Liu et al., 2015) and significant surface (Johnston et al., 2021) and subsurface warming (Steinberg et al., 2024) could considerably alter the eddy field and thermal characteristics of eddies in the future. Climate projections for tropical waters (0–200 m) reveal an extensive shoaling of the MLD (Lesser & Slattery, 2020) due to increases in SSTs and a reduction of winds (Alexander et al., 2018; Behrenfeld et al., 2006; Capotondi et al., 2012; Gittings et al., 2018; Lesser & Slattery, 2020; Signorini et al., 2015). Increased shoaling of the MLD over FGBNMS could change the monthly variability that contributes to the important exchange of water chemistry over this unique reef environment. Alternatively, mesophotic reefs below the mixed layer could be protected from SST anomalies at the surface under increased warming (Diaz et al., 2023; McWhorter et al., 2024). Projected changes to ocean conditions surrounding FGBNMS due to climate change are multifaceted, including increases in stratification, sea surface and subsurface temperatures, ocean acidification, hypoxia, and a potential weakening of the Loop Current resulting in a possible change in the eddy field.

## 5. Conclusion

The environmental variability introduced by eddy interactions result in alterations to temperature, salinity, and MLD, which have in turn potentially promoted the resiliency of the coral reef ecosystem within FGBNMS. The seasonal variability of the mixed layer coupled with eddy conditions proves important for understanding temperature and salinity variability over this relatively pristine coral reef ecosystem. Eddy days have been quantified to persist in the area at least half of each month, either anticyclonic or cyclonic eddies. While these eddies are relatively weaker than the eddies in the rest of the surrounding Gulf of Mexico, they contribute to major water column exchanges over the mesophotic reef environment that modulate seasonal and long-term climate variability. The largest differences in temperature between anticyclonic and cyclonic eddies occur during the months of August to November when amplified warming has the most potential to influence corals associated with warm summertime temperatures. Our assessment does not indicate a clear link between eddy influence (specifically anticyclonic eddy amplified warming) and recent bleaching event years over FGBNMS, demonstrating the importance of the frequency and amplitude of both anticyclonic and cyclonic eddies in this region. As an indication of subsurface warming, our satellite analysis shows thermal increases in wintertime cyclonic eddies in recent years. Our method connecting open ocean observations to the shelf-edge using Argo temperature and salinity observations is foundational to expanding the analysis of eddy influence on biogeochemistry over FGBNMS using an increasing number of BGC-Argo observations in the Gulf of Mexico. Given that some projections reveal a weakening of the Loop Current under climate change, the eddy field surrounding the FGBNMS region will likely be altered, emphasizing the value of establishing a physical and biogeochemical baseline that can be assessed within the context of future change.

## Conflict of Interest

The authors declare no conflicts of interest relevant to this study.

## Data Availability Statement

These data were collected and made freely available by the International Argo Program and the national programs that contribute to it. The Argo Program is part of the Global Ocean Observing System (Argo, 2020). Copernicus Marine Environmental Monitoring Service L4 SLA and geostrophic currents were obtained from 1 September 2002 through 31 July 2022 from Copernicus.eu ([https://data.marine.copernicus.eu/product/SEALEVEL\\_GLO\\_PHY\\_L4\\_MY\\_008\\_047/description](https://data.marine.copernicus.eu/product/SEALEVEL_GLO_PHY_L4_MY_008_047/description)). NOAA Geo-Polar sea surface temperature data (Maturi et al., 2017) was obtained via NOAA CoastWatch and is available from 1 September 2002 through 31 July 2022 at <https://coastwatch.noaa.gov/cw/satellite-data-products/sea-surface-temperature/sea-surface-temperature-near-real-time-geopolar-blended.html>. Code and data are available, (<https://doi.org/10.5281/zenodo.11429807>).

**Acknowledgments**

This research would not have been possible without the foundation of the Argo network and the many contributors to this invaluable dataset. The content is solely the responsibility of the authors and does not necessarily represent the official views of the Gulf of Mexico Research Program or the National Academies of Sciences, Engineering, and Medicine. Disclaimer: the scientific results and conclusions, as well as any views or opinions expressed herein, are those of the authors and do not necessarily reflect those of NOAA or the Department of Commerce. Support for this analysis was provided by NOAA's Atlantic Oceanographic and Meteorological Laboratory (AOML) and Global Ocean Monitoring and Observing. Contributions made by H. Roman-Stock were supported under Grants ST13301CQ0050/1332KP22FNEED0042. H. Frenzel was funded by the Cooperative Institute for Climate, Ocean, and Ecosystem Studies, a cooperative institute of the University of Washington and NOAA, (agreement NA20OAR4320271, Contribution No. 2023-1328). Pacific Marine Environmental Laboratory contribution number 5582. M. Le Hénaff received partial support for work on this publication by AOML and was supported in part under the auspices of the Cooperative Institute for Marine and Atmospheric Studies, a cooperative institute of the University of Miami and NOAA (agreement NA20OAR4320472). Research reported in this publication was partly supported by the Gulf of Mexico Research Program of the National Academies of Sciences, Engineering, and Medicine under award number 2000013149.

**References**

Aeby, G. S., Ushijima, B., Campbell, J. E., Jones, S., Williams, G. J., Meyer, J. L., et al. (2019). Pathogenesis of a tissue loss disease affecting multiple species of corals along the Florida Reef Tract. *Frontiers in Marine Science*, 6, 678. <https://doi.org/10.3389/fmars.2019.00678>

Alexander, M. A., Scott, J. D., Friedland, K. D., Mills, K. E., Nye, J. A., Pershing, A. J., & Thomas, A. C. (2018). Projected sea surface temperatures over the 21st century: Changes in the mean, variability and extremes for large marine ecosystem regions of Northern Oceans. *Elementa: Science of the Anthropocene*, 6, 9. <https://doi.org/10.1525/elementa.191>

Altieri, A. H., Harrison, S. B., Seemann, J., Collin, R., Diaz, R. J., & Knowlton, N. (2017). Tropical dead zones and mass mortalities on coral reefs. *Proceedings of the National Academy of Sciences*, 114(14), 3660–3665. <https://doi.org/10.1073/pnas.1621517114>

Argo (2020). Argo float data and metadata from Global Data Assembly Centre (Argo GDAC) – Snapshot of Argo GDAC of August 2020 [Dataset]. *SEANOE*. <https://doi.org/10.17882/42182#76230>

Behrenfeld, M. J., Worthington, K., Sherrell, R. M., Chavez, F. P., Strutton, P., McPhaden, M., & Shea, D. M. (2006). Controls on tropical Pacific Ocean productivity revealed through nutrient stress diagnostics. *Nature*, 442(7106), 1025–1028. <https://doi.org/10.1038/nature05083>

Brainerd, K. E., & Gregg, M. C. (1995). Surface mixed and mixing layer depths. *Deep Sea Research Part I: Oceanographic Research Papers*, 42(9), 1521–1543. [https://doi.org/10.1016/0967-0637\(95\)00068-h](https://doi.org/10.1016/0967-0637(95)00068-h)

Bright, T. J., & Gittings, S. R. (2023). Geological faulting a possible trigger for brine-induced reef mortality at East Flower Garden Bank, NW Gulf of Mexico. *Bulletin of Marine Science*, 99(1), 57–64. <https://doi.org/10.5343/bms.2022.0024>

Brokaw, R. J., Subrahmanyam, B., Trott, C. B., & Chaigneau, A. (2020). Eddy surface characteristics and vertical structure in the Gulf of Mexico from satellite observations and model simulations. *Journal of Geophysical Research: Oceans*, 125(2), e2019JC015538. <https://doi.org/10.1029/2019jc015538>

Capotondi, A., Alexander, M. A., Bond, N. A., Curchitser, E. N., & Scott, J. D. (2012). Enhanced upper ocean stratification with climate change in the CMIP3 models. *Journal of Geophysical Research*, 117(C4), C04031. <https://doi.org/10.1029/2011jc007409>

Chaigneau, A., Eldin, G., & Dewitte, B. (2009). Eddy activity in the four major upwelling systems from satellite altimetry (1992–2007). *Progress in Oceanography*, 83(1–4), 117–123. <https://doi.org/10.1016/j.pocean.2009.07.012>

Chaigneau, A., Gizolme, A., & Grados, C. (2008). Mesoscale eddies off Peru in altimeter records: Identification algorithms and eddy spatio-temporal patterns. *Progress in Oceanography*, 79(2–4), 106–119. <https://doi.org/10.1016/j.pocean.2008.10.013>

Chelton, D. B., Gaube, P., Schlax, M. G., Early, J. J., & Samelson, R. M. (2011). The influence of nonlinear mesoscale eddies on near-surface oceanic chlorophyll. *Science*, 334(6054), 328–332. <https://doi.org/10.1126/science.1208897>

Cornec, M., Huang, Y., Jutard, Q., Sauzède, R., & Schmechtig, C. (2022). OneArgo-R: An R toolbox for accessing and visualizing Argo data (v1.0.1) [Dataset]. *Zenodo*. <https://doi.org/10.5281/zenodo.6604735>

Courtney, T. A., Lebrato, M., Bates, N. R., Collins, A., De Putron, S. J., Garley, R., et al. (2017). Environmental controls on modern scleractinian coral and reef-scale calcification. *Science Advances*, 3(11), e1701356. <https://doi.org/10.1126/sciadv.1701356>

Cróquer, A., Weil, E., & Rogers, C. S. (2021). Similarities and differences between two deadly Caribbean coral diseases: White plague and stony coral tissue loss disease. *Frontiers in Marine Science*, 8, 709544. <https://doi.org/10.3389/fmars.2021.709544>

Dawson, H. R., Strutton, P. G., & Gaube, P. (2018). The unusual surface chlorophyll signatures of Southern Ocean eddies. *Journal of Geophysical Research: Oceans*, 123(9), 6053–6069. <https://doi.org/10.1029/2017jc013628>

de Boyer Montégut, C., Madec, G., Fischer, A. S., Lazar, A., & Iudicone, D. (2004). Mixed layer depth over the global ocean: An examination of profile data and a profile-based climatology. *Journal of Geophysical Research*, 109(C12), C12003. <https://doi.org/10.1029/2004jc002378>

de Lanza Espino, G., Gómez-Rojas, J. C., Pisanty, I., Ezcurra, E., Whithers, K., & Nipper, M. (2004). Physical and chemical characteristics of the Gulf of Mexico. In *Environmental analysis of the Gulf of Mexico* (1) (pp. 41–61). DF Harte Research Institute for Gulf of Mexico Studies Special Publication Series.

Diaz, C., Foster, N. L., Attrill, M. J., Bolton, A., Ganderton, P., Howell, K. L., et al. (2023). Mesophotic coral bleaching associated with changes in thermocline depth. *Nature Communications*, 14(1), 6528. <https://doi.org/10.1038/s41467-023-42279-2>

Domingues, R., Goni, G., Bringas, F., Muhling, B., Lindo-Atchati, D., & Walter, J. (2016). Variability of preferred environmental conditions for Atlantic bluefin tuna (*Thunnus thynnus*) larvae in the Gulf of Mexico during 1993–2011. *Fisheries Oceanography*, 25(3), 320–336. <https://doi.org/10.1111/fog.12152>

Ducet, N., Le Traon, P.-Y., & Reverdin, G. (2000). Global high-resolution mapping of ocean circulation from TOPEX/Poseidon and ERS-1 and-2. *Journal of Geophysical Research*, 105(C8), 19477–19498. <https://doi.org/10.1029/2000jc900063>

Eakin, C. M., Morgan, J. A., Heron, S. F., Smith, T. B., Liu, G., Alvarez-Filip, L., et al. (2010). Caribbean corals in crisis: Record thermal stress, bleaching, and mortality in 2005. *PLoS One*, 5(11), e13969. <https://doi.org/10.1371/journal.pone.0013969>

Etnoyer, P., Bassett, R., Adams, C., Battista, T., Blakeway, R., Harter, S., et al. (2021). NOAA deep sea coral research and technology program southeast deep coral initiative (SEDCI) 2016–2019.

Falkowski, P. G., Ziemann, D., Kolber, Z., & Bienfang, P. K. (1991). Role of eddy pumping in enhancing primary production in the ocean. *Nature*, 352(6330), 55–58. <https://doi.org/10.1038/352055a0>

Frenzel, H., Sharp, J. D., Fassbender, A. J., & Buzby, N. (2022). OneArgo-Mat: A MATLAB toolbox for accessing and visualizing Argo data (version v1.0.2) [Dataset]. *Zenodo*. <https://doi.org/10.5281/zenodo.6799431>

Gittings, J. A., Raitos, D. E., Krokos, G., & Hoteit, I. (2018). Impacts of warming on phytoplankton abundance and phenology in a typical tropical marine ecosystem. *Scientific Reports*, 8(1), 2240. <https://doi.org/10.1038/s41598-018-20560-5>

González-Espinoza, P. C., & Donner, S. D. (2020). Predicting cold-water bleaching in corals: Role of temperature, and potential integration of light exposure. *Marine Ecology Progress Series*, 642, 133–146. <https://doi.org/10.3354/meps13336>

Gordon, A. L. (1967). Circulation of the Caribbean Sea. *Journal of Geophysical Research*, 72(24), 6207–6223. <https://doi.org/10.1029/jz072i024p06207>

Greaser, S. R., Subrahmanyam, B., Trott, C. B., & Roman-Stork, H. L. (2020). Interactions between mesoscale eddies and synoptic oscillations in the Bay of Bengal during the strong monsoon of 2019. *Journal of Geophysical Research: Oceans*, 125(10), e2020JC016772. <https://doi.org/10.1029/2020jc016772>

Hamilton, P., Berger, T. J., & Johnson, W. (2002). On the structure and motions of cyclones in the northern Gulf of Mexico. *Journal of Geophysical Research*, 107(C12), 1-1–1-18. <https://doi.org/10.1029/1999jc000270>

Hoegh-Guldberg, O., Mumby, P. J., Hooten, A. J., Steneck, R. S., Greenfield, P., Gomez, E., et al. (2007). Coral reefs under rapid climate change and ocean acidification. *Science*, 318(5857), 1737–1742. <https://doi.org/10.1126/science.1152509>

Holte, J., & Talley, L. (2009). A new algorithm for finding mixed layer depths with applications to Argo data and Subantarctic Mode Water formation. *Journal of Atmospheric and Oceanic Technology*, 26(9), 1920–1939. <https://doi.org/10.1175/2009jtech0543.1>

- Hughes, T. P., Anderson, K. D., Connolly, S. R., Heron, S. F., Kerry, J. T., Lough, J. M., et al. (2018). Spatial and temporal patterns of mass bleaching of corals in the Anthropocene. *Science*, 359(6371), 80–83. <https://doi.org/10.1126/science.aan8048>
- Jackson, J. B. C., Donovan, M. K., Cramer, K. L., & Lam, V. V. (2014). Status and trends of Caribbean coral reefs. In *Global coral reef monitoring network* (pp. 1970–2012). IUCN.
- Johnson, M. D., Scott, J. J., Leray, M., Lucey, N., Bravo, L. M. R., Wied, W. L., & Altieri, A. H. (2021). Rapid ecosystem-scale consequences of acute deoxygenation on a Caribbean coral reef. *Nature Communications*, 12(1), 4522. <https://doi.org/10.1038/s41467-021-24777-3>
- Johnston, M. A., Embesi, J. A., Eckert, R. J., Nuttall, M. F., Hickerson, E. L., & Schmahl, G. P. (2016). Persistence of coral assemblages at east and west flower garden banks, gulf of Mexico. *Coral Reefs*, 35(3), 821–826. <https://doi.org/10.1007/s00338-016-1452-x>
- Johnston, M. A., Hickerson, E. L., Nuttall, M. F., Blakeway, R. D., Sterne, T. K., Eckert, R. J., & Schmahl, G. P. (2019). Coral bleaching and recovery from 2016 to 2017 at East and West Flower Garden Banks, Gulf of Mexico. *Coral Reefs*, 38(4), 787–799. <https://doi.org/10.1007/s00338-019-01788-7>
- Johnston, M. A., Nuttall, M. F., Eckert, R. J., Blakeway, R. D., Sterne, T. K., Hickerson, E. L., et al. (2019). Localized coral reef mortality event at east flower garden bank, Gulf of Mexico. *Bulletin of Marine Science*, 95(2), 239–250. <https://doi.org/10.5343/bms.2018.0057>
- Johnston, M. A., O'Connell, K., Blakeway, R. D., MacMillan, J., Nuttall, M. F., Hu, X., et al. (2021). *Long-term monitoring at East and West Flower garden banks: 2019 annual report (annual report no. ONMS-21-02)* (p. 88). U.S. Department of Commerce, National Oceanic and Atmospheric Administration, Flower Garden Banks National Marine Sanctuary.
- Johnston, M. A., Studivan, M. S., Enochs, I. C., Correa, A., Besemer, N., Eckert, R. J., et al. (2023). Coral disease outbreak at the remote Flower Garden Banks, Gulf of Mexico. *Frontiers in Marine Science*, 10, 100. <https://doi.org/10.3389/fmars.2023.1111749>
- Kara, A. B., Rochford, P. A., & Hurlburt, H. E. (2003). Mixed layer depth variability over the global ocean. *Journal of Geophysical Research*, 108(C3), 3079. <https://doi.org/10.1029/2000jc000736>
- Kealoha, A. K., Doyle, S. M., Shamberger, K. E., Sylvan, J. B., Hetland, R. D., & DiMarco, S. F. (2020). Localized hypoxia may have caused coral reef mortality at the Flower Garden Banks. *Coral Reefs*, 39(1), 119–132. <https://doi.org/10.1007/s00338-019-01883-9>
- Kelley, D. E., Harbin, J., & Richards, C. (2021). argoFloats: An R package for analyzing Argo data. *Frontiers in Marine Science*, 8, 635922. <https://doi.org/10.3389/fmars.2021.635922>
- Kleypas, J. A., McManus, J. W., & Meñez, L. A. (1999). Environmental limits to coral reef development: Where do we draw the line? *American Zoologist*, 39(1), 146–159. <https://doi.org/10.1093/icb/39.1.146>
- Le Hénaff, M., Kourafalou, V. H., Dussurget, R., & Lumpkin, R. (2014). Cyclonic activity in the eastern Gulf of Mexico: Characterization from along-track altimetry and in situ drifter trajectories. *Progress in Oceanography*, 120, 120–138. <https://doi.org/10.1016/j.pocean.2013.08.002>
- Le Hénaff, M., Muller-Karger, F. E., Kourafalou, V. H., Otis, D., Johnson, K. A., McEachron, L., & Kang, H. (2019). Coral mortality event in the Flower Garden Banks of the Gulf of Mexico in July 2016: Local hypoxia due to cross-shelf transport of coastal flood waters? *Continental Shelf Research*, 190, 103988. <https://doi.org/10.1016/j.csr.2019.103988>
- Lesser, M. P., & Slattery, M. (2020). Will coral reef sponges be winners in the Anthropocene? *Global Change Biology*, 26(6), 3202–3211. <https://doi.org/10.1111/gcb.15039>
- Le Traon, P. Y., Nadal, F., & Ducet, N. (1998). An improved mapping method of multisatellite altimeter data. *Journal of Atmospheric and Oceanic Technology*, 15(2), 522–534. [https://doi.org/10.1175/1520-0426\(1998\)015<0522:aimmom>2.0.co;2](https://doi.org/10.1175/1520-0426(1998)015<0522:aimmom>2.0.co;2)
- Limer, B. D., Bloomberg, J., & Holstein, D. M. (2020). The influence of eddies on coral larval retention in the Flower Garden Banks. *Frontiers in Marine Science*, 7, 372. <https://doi.org/10.3389/fmars.2020.00372>
- Liu, Y., Lee, S.-K., Enfield, D. B., Muhling, B. A., Lamkin, J. T., Muller-Karger, F. E., & Roffer, M. A. (2015). Potential impact of climate change on the Intra-Americas Sea: Part-1. A dynamic downscaling of the CMIP5 model projections. *Journal of Marine Systems*, 148, 56–69. <https://doi.org/10.1016/j.jmarsys.2015.01.007>
- Lugo-Fernández, A., Deslarzes, K. J., Price, J. M., Boland, G. S., & Morin, M. V. (2001). Inferring probable dispersal of Flower Garden Banks coral larvae (Gulf of Mexico) using observed and simulated drifter trajectories. *Continental Shelf Research*, 21(1), 47–67. [https://doi.org/10.1016/s0278-4343\(00\)00072-8](https://doi.org/10.1016/s0278-4343(00)00072-8)
- Manzello, D. P., Kolodziej, G., Kirkland, A., Besemer, N., & Enochs, I. C. (2021). Increasing coral calcification in *Orbicella faveolata* and *Pseudodiploria strigosa* at Flower Garden Banks, Gulf of Mexico. *Coral Reefs*, 40(4), 1097–1111. <https://doi.org/10.1007/s00338-021-02108-8>
- Mason, E., Pascual, A., & McWilliams, J. C. (2014). A new sea surface height-based code for oceanic mesoscale eddy tracking. *Journal of Atmospheric and Oceanic Technology*, 31(5), 1181–1188. <https://doi.org/10.1175/jtech-d-14-00019.1>
- Maturi, E., Harris, A., Mittaz, J., Sapper, J., Wick, G., Zhu, X., & Koner, P. (2017). A new high-resolution sea surface temperature blended analysis. *Bulletin of the American Meteorological Society*, 98(5), 1015–1026. <https://doi.org/10.1175/bams-d-15-00002.1>
- McGillicuddy, D. J., Jr., Robinson, A. R., Siegel, D. A., Jannasch, H. W., Johnson, R., Dickey, T. D., et al. (1998). Influence of mesoscale eddies on new production in the Sargasso Sea. *Nature*, 394(6690), 263–266. <https://doi.org/10.1038/28367>
- McGillicuddy Jr, D. J. (2016). Mechanisms of physical-biological-biochemical interaction at the oceanic mesoscale. *Annual Review of Marine Science*, 8(1), 125–159. <https://doi.org/10.1146/annurev-marine-010814-015606>
- McWhorter, J. K., Halloran, P. R., Roff, G., & Mumby, P. J. (2024). Climate change impacts on mesophotic regions of the Great Barrier Reef. *Proceedings of the National Academy of Sciences*, 121(16), e2303336121. <https://doi.org/10.1073/pnas.2303336121>
- Moreau, S., Penna, A. D., Llort, J., Patel, R., Langlais, C., Boyd, P. W., et al. (2017). Eddy-induced carbon transport across the Antarctic Circumpolar Current. *Global Biogeochemical Cycles*, 31(9), 1368–1386. <https://doi.org/10.1002/2017gb005669>
- Muller, E. M., Sartor, C., Alcaraz, N. I., & Van Woessik, R. (2020). Spatial epidemiology of the stony-coral-tissue-loss disease in Florida. *Frontiers in Marine Science*, 7, 163. <https://doi.org/10.3389/fmars.2020.00163>
- Patel, R. S., Llort, J., Stratton, P. G., Phillips, H. E., Moreau, S., Conde Pardo, P., & Lenton, A. (2020). The biogeochemical structure of Southern Ocean mesoscale eddies. *Journal of Geophysical Research: Oceans*, 125(8), e2020JC016115. <https://doi.org/10.1029/2020jc016115>
- Pegliasco, C., Chaigneau, A., & Morrow, R. (2015). Main eddy vertical structures observed in the four major Eastern Boundary Upwelling Systems. *Journal of Geophysical Research: Oceans*, 120(9), 6008–6033. <https://doi.org/10.1002/2015jc010950>
- Rezak, R., Bright, T. J., & McGrail, D. W. (1985). Reefs and banks of the northwestern Gulf of Mexico: Their geological, biological, and physical dynamics. (No Title).
- Roman-Stork, H. L., Byrne, D. A., & Leuliette, E. W. (2023). MESI: A multiparameter eddy significance index. *Earth and Space Science*, 10(2), e2022EA002583. <https://doi.org/10.1029/2022ea002583>
- Roman-Stork, H. L., Subrahmanyam, B., & Murty, V. S. N. (2019). Quasi-biweekly oscillations in the Bay of Bengal in observations and model simulations. *Deep Sea Research Part II: Topical Studies in Oceanography*, 168, 104609. <https://doi.org/10.1016/j.dsr2.2019.06.017>
- Scharroo, R., Leuliette, E., Lillibridge, J., Byrne, D., Naeije, M., & Mitchum, G. (2013). RAD5: Consistent multi-mission products. In *20 years of progress in radar altimetry* (Vol. 710).

- Siegel, D. A., McGillicuddy Jr, D. J., & Fields, E. A. (1999). Mesoscale eddies, satellite altimetry, and new production in the Sargasso Sea. *Journal of Geophysical Research*, *104*(C6), 13359–13379. <https://doi.org/10.1029/1999jc900051>
- Siegel, D. A., Peterson, P., McGillicuddy Jr, D. J., Maritorena, S., & Nelson, N. B. (2011). Bio-optical footprints created by mesoscale eddies in the Sargasso Sea. *Geophysical Research Letters*, *38*(13), L13608. <https://doi.org/10.1029/2011gl047660>
- Signorini, S. R., Franz, B. A., & McClain, C. R. (2015). Chlorophyll variability in the oligotrophic gyres: Mechanisms, seasonality and trends. *Frontiers in Marine Science*, *2*, 1. <https://doi.org/10.3389/fmars.2015.00001>
- Skirving, W., Heron, S. F., Marsh, B. L., Liu, G., De La Cour, J. L., Geiger, E. F., & Eakin, C. M. (2019). The relentless march of mass coral bleaching: A global perspective of changing heat stress. *Coral Reefs*, *38*(4), 547–557. <https://doi.org/10.1007/s00338-019-01799-4>
- Spring, D. L., & Williams, G. J. (2023). Influence of upwelling on coral reef benthic communities: A systematic review and meta-analysis. *Proceedings of the Royal Society B*, *290*(1995), 20230023. <https://doi.org/10.1098/rspb.2023.0023>
- Steinberg, J. M., Piecuch, C. G., Hamlington, B. D., Thompson, P. R., & Coats, S. (2024). Influence of deep-ocean warming on coastal sea-level decadal trends in the Gulf of Mexico. *Journal of Geophysical Research: Oceans*, *129*(1), e2023JC019681. <https://doi.org/10.1029/2023jc019681>
- Strutton, P. G., Trull, T. W., Phillips, H. E., Duran, E. R., & Pump, S. (2023). Biogeochemical Argo floats reveal the evolution of subsurface chlorophyll and particulate organic carbon in southeast Indian Ocean eddies. *Journal of Geophysical Research: Oceans*, *128*(4), e2022JC018984. <https://doi.org/10.1029/2022jc018984>
- Sturges, W., & Evans, J. C. (1983). On the variability of the Loop Current in the Gulf of Mexico. *Journal of Marine Research*, *41*(4), 639–653. <https://doi.org/10.1357/002224083788520487>
- Suga, T., Motoki, K., Aoki, Y., & Macdonald, A. M. (2004). The North Pacific climatology of winter mixed layer and mode waters. *Journal of Physical Oceanography*, *34*(1), 3–22. [https://doi.org/10.1175/1520-0485\(2004\)034<0003:tnpcow>2.0.co;2](https://doi.org/10.1175/1520-0485(2004)034<0003:tnpcow>2.0.co;2)
- Taburet, G., Sanchez-Roman, A., Ballarotta, M., Pujol, M.-I., Legeais, J.-F., Fournier, F., et al. (2019). DUACS DT2018: 25 years of reprocessed sea level altimetry products. *Ocean Science*, *15*(5), 1207–1224. <https://doi.org/10.5194/os-15-1207-2019>
- Teague, W. J., Wijesekera, H. W., Jarosz, E., Fribance, D. B., Lugo-Fernández, A., & Hallock, Z. R. (2013). Current and hydrographic conditions at the East Flower Garden Bank in 2011. *Continental Shelf Research*, *63*, 43–58. <https://doi.org/10.1016/j.csr.2013.04.039>
- Trott, C. B., Subrahmanyam, B., Chaigneau, A., & Roman-Stork, H. L. (2019). Eddy-induced temperature and salinity variability in the Arabian Sea. *Geophysical Research Letters*, *46*(5), 2734–2742. <https://doi.org/10.1029/2018gl081605>
- Wong, A., Keeley, R., & Carval, T. (2022). Argo quality control manual for CTD and trajectory data.
- Wong, A. P., Wijffels, S. E., Riser, S. C., Pouliquen, S., Hosoda, S., Roemmich, D., et al. (2020). Argo data 1999–2019: Two million temperature-salinity profiles and subsurface velocity observations from a global array of profiling floats. *Frontiers in Marine Science*, *7*, 700. <https://doi.org/10.3389/fmars.2020.00700>
- Wyatt, A. S., Leichter, J. J., Washburn, L., Kui, L., Edmunds, P. J., & Burgess, S. C. (2023). Hidden heatwaves and severe coral bleaching linked to mesoscale eddies and thermocline dynamics. *Nature Communications*, *14*(1), 25. <https://doi.org/10.1038/s41467-022-35550-5>
- Xu, Z., Han, Y., & Yang, Z. (2019). Dynamical downscaling of regional climate: A review of methods and limitations. *Science China Earth Sciences*, *62*(2), 365–375. <https://doi.org/10.1007/s11430-018-9261-5>
- Zavala-Hidalgo, J., Morey, S. L., & O'Brien, J. J. (2003). Cyclonic eddies northeast of the Campeche Bank from altimetry data. *Journal of Physical Oceanography*, *33*(3), 623–629. [https://doi.org/10.1175/1520-0485\(2003\)033<0623:cenot>2.0.co;2](https://doi.org/10.1175/1520-0485(2003)033<0623:cenot>2.0.co;2)